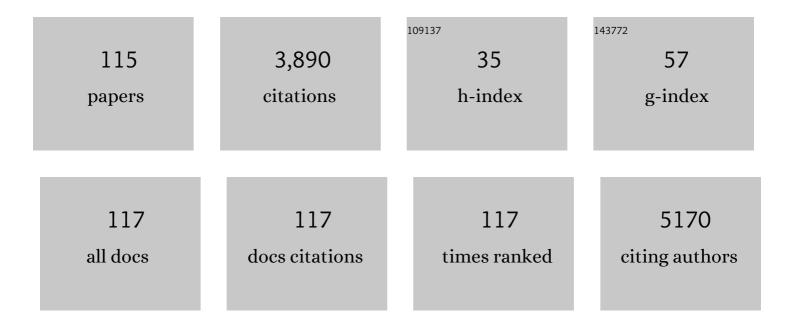
## Chris S Blackman

List of Publications by Year in descending order

Source: https://exaly.com/author-pdf/7516201/publications.pdf Version: 2024-02-01



CHDIS S RIACKMAN

#	Article	IF	CITATIONS
1	Au nanoparticle-functionalised WO <sub>3</sub> nanoneedles and their application in high sensitivity gas sensor devices. Chemical Communications, 2011, 47, 565-567.	2.2	204
2	Recent Advances in 2D Inorganic Nanomaterials for SERS Sensing. Advanced Materials, 2019, 31, e1803432.	11.1	184
3	Atmospheric Pressure Chemical Vapor Deposition of Crystalline Monoclinic WO3 and WO3-x Thin Films from Reaction of WCl6 with O-Containing Solvents and Their Photochromic and Electrochromic Properties. Chemistry of Materials, 2005, 17, 1583-1590.	3.2	161
4	Singleâ€Step Deposition of Au†and Ptâ€Nanoparticleâ€Functionalized Tungsten Oxide Nanoneedles Synthesized Via Aerosolâ€Assisted CVD, and Used for Fabrication of Selective Gas Microsensor Arrays. Advanced Functional Materials, 2013, 23, 1313-1322.	7.8	143
5	Facile synthesis of mesoporous hierarchical Co <sub>3</sub> O <sub>4</sub> –TiO <sub>2</sub> p–n heterojunctions with greatly enhanced gas sensing performance. Journal of Materials Chemistry A, 2017, 5, 10387-10397.	5.2	116
6	Evidence and Effect of Photogenerated Charge Transfer for Enhanced Photocatalysis in WO <sub>3</sub> /TiO <sub>2</sub> Heterojunction Films: A Computational and Experimental Study. Advanced Functional Materials, 2017, 27, 1605413.	7.8	115
7	Atmospheric pressure chemical vapour deposition of thermochromic tungsten doped vanadium dioxide thin films for use in architectural glazing. Thin Solid Films, 2009, 517, 4565-4570.	0.8	111
8	Water Oxidation and Electron Extraction Kinetics in Nanostructured Tungsten Trioxide Photoanodes. Journal of the American Chemical Society, 2018, 140, 16168-16177.	6.6	105
9	Effect of oxygen deficiency on the excited state kinetics of WO <sub>3</sub> and implications for photocatalysis. Chemical Science, 2019, 10, 5667-5677.	3.7	97
10	APCVD of thermochromic vanadium dioxide thin films—solid solutions V2–xMxO2 (M = Mo, Nb) or composites VO2 : SnO2. Journal of Materials Chemistry, 2005, 15, 4560.	6.7	93
11	Aerosol-Assisted CVD-Grown PdO Nanoparticle-Decorated Tungsten Oxide Nanoneedles Extremely Sensitive and Selective to Hydrogen. ACS Applied Materials & Interfaces, 2016, 8, 10413-10421.	4.0	93
12	A simple, low-cost CVD route to thin films of BiFeO3 for efficient water photo-oxidation. Journal of Materials Chemistry A, 2014, 2, 2922.	5.2	89
13	Gold clusters on WO3 nanoneedles grown via AACVD: XPS and TEM studies. Materials Chemistry and Physics, 2012, 134, 809-813.	2.0	83
14	Optimizing the Activity of Nanoneedle Structured WO <sub>3</sub> Photoanodes for Solar Water Splitting: Direct Synthesis via Chemical Vapor Deposition. Journal of Physical Chemistry C, 2017, 121, 5983-5993.	1.5	71
15	Aerosol assisted chemical vapour deposition of WO3 thin films from tungsten hexacarbonyl and their gas sensing properties. Journal of Materials Chemistry, 2007, 17, 3708.	6.7	64
16	Atmospheric pressure chemical vapour deposition of vanadium diselenide thin films. Applied Surface Science, 2007, 253, 6041-6046.	3.1	64
17	Dynamics of Photoâ€Induced Surface Oxygen Vacancies in Metalâ€Oxide Semiconductors Studied Under Ambient Conditions. Advanced Science, 2019, 6, 1901841.	5.6	62
18	Tantalum and Titanium doped In <sub>2</sub> O <sub>3</sub> Thin Films by Aerosol-Assisted Chemical Vapor Deposition and their Gas Sensing Properties. Chemistry of Materials, 2012, 24, 2864-2871.	3.2	61

#	Article	IF	CITATIONS
19	MOCVD of crystalline Bi2O3 thin films using a single-source bismuth alkoxide precursor and their use in photodegradation of water. Journal of Materials Chemistry, 2010, 20, 7881.	6.7	59
20	WO <sub>3</sub> /BiVO <sub>4</sub> : impact of charge separation at the timescale of water oxidation. Chemical Science, 2019, 10, 2643-2652.	3.7	59
21	Aerosol-assisted chemical vapour deposition of WO3 thin films using polyoxometallate precursors and their gas sensing properties. Journal of Materials Chemistry, 2007, 17, 1063.	6.7	57
22	Aerosol assisted chemical vapour deposition of MoO3 and MoO2 thin films on glass from molybdenum polyoxometallate precursors; thermophoresis and gas phase nanoparticle formation. Journal of Materials Chemistry, 2006, 16, 3575.	6.7	55
23	Visible-light driven water splitting over BiFeO <sub>3</sub> photoanodes grown via the LPCVD reaction of [Bi(O <sup>t</sup> Bu) <sub>3</sub> ] and [Fe(O <sup>t</sup> Bu) <sub>3</sub> ] <sub>2</sub> and enhanced with a surface nickel oxygen evolution catalyst. Nanoscale. 2015. 7. 16343-16353.	2.8	55
24	Micromachined gas sensors based on tungsten oxide nanoneedles directly integrated via aerosol assisted CVD. Sensors and Actuators B: Chemical, 2014, 198, 210-218.	4.0	53
25	Chemical Vapour Deposition of Gas Sensitive Metal Oxides. Chemosensors, 2016, 4, 4.	1.8	52
26	Self-standing electrodes with core-shell structures for high-performance supercapacitors. Energy Storage Materials, 2017, 9, 119-125.	9.5	52
27	An array of WO <sub>3</sub> and CTO heterojunction semiconducting metal oxide gas sensors used as a tool for explosive detection. Journal of Materials Chemistry A, 2017, 5, 2172-2179.	5.2	50
28	Resonant Ta Doping for Enhanced Mobility in Transparent Conducting SnO <sub>2</sub> . Chemistry of Materials, 2020, 32, 1964-1973.	3.2	50
29	The Effect of Film Thickness on the Gas Sensing Properties of Ultra-Thin TiO2 Films Deposited by Atomic Layer Deposition. Sensors, 2018, 18, 735.	2.1	49
30	Thermochromic Coatings for Intelligent Architectural Glazing. Journal of Nano Research, 0, 2, 1-20.	0.8	46
31	Nanostructured tungsten oxide gas sensors prepared by electric field assisted aerosol assisted chemical vapour deposition. Journal of Materials Chemistry A, 2013, 1, 1827-1833.	5.2	43
32	ZnO Rods with Exposed {100} Facets Grown via a Self-Catalyzed Vapor–Solid Mechanism and Their Photocatalytic and Gas Sensing Properties. ACS Applied Materials & Interfaces, 2016, 8, 33335-33342.	4.0	42
33	Important considerations for effective gas sensors based on metal oxide nanoneedles films. Sensors and Actuators B: Chemical, 2012, 161, 406-413.	4.0	39
34	Humidity-Tolerant Ultrathin NiO Gas-Sensing Films. ACS Sensors, 2020, 5, 1389-1397.	4.0	38
35	Aerosol assisted chemical vapour deposition of gas sensitive SnO2 and Au-functionalised SnO2 nanorods via a non-catalysed vapour solid (VS) mechanism. Scientific Reports, 2016, 6, 28464.	1.6	37
36	Aerosol Assisted Chemical Vapour Deposition Control Parameters for Selective Deposition of Tungsten Oxide Nanostructures. Journal of Nanoscience and Nanotechnology, 2011, 11, 8214-8220.	0.9	36

#	Article	IF	CITATIONS
37	Growth mechanism of planar or nanorod structured tungsten oxide thin films deposited via aerosol assisted chemical vapour deposition (AACVD). Physica Status Solidi C: Current Topics in Solid State Physics, 2015, 12, 869-877.	0.8	36
38	The APCVD of tungsten oxide thin films from reaction of WCl6 with ethanol and results on their gas-sensing properties. Polyhedron, 2007, 26, 1493-1498.	1.0	34
39	Photocatalytic activity of needle-like TiO2/WO3â^'x thin films prepared by chemical vapour deposition. Journal of Photochemistry and Photobiology A: Chemistry, 2012, 239, 60-64.	2.0	34
40	The gas-sensing properties of WO3â^'xthin films deposited via the atmospheric pressure chemical vapour deposition (APCVD) of WCl6with ethanol. Measurement Science and Technology, 2008, 19, 025203.	1.4	31
41	Synthesis of Zirconium Guanidinate Complexes and the Formation of Zirconium Carbonitride via Low Pressure CVD. Organometallics, 2009, 28, 1838-1844.	1.1	30
42	Microsensors based on Pt–nanoparticle functionalised tungsten oxide nanoneedles for monitoring hydrogen sulfide. RSC Advances, 2014, 4, 1489-1495.	1.7	30
43	Solution Processing of GaAs Thin Films for Photovoltaic Applications. Chemistry of Materials, 2014, 26, 4419-4424.	3.2	29
44	Tin phosphide coatings from the atmospheric pressure chemical vapour deposition of SnX4 (X=Cl or) Tj ETQq0 0	0 rgBT /O	verlock 10 Tf
45	Development of a HS-SPME/GC–MS method for the analysis of volatile organic compounds from fabrics for forensic reconstruction applications. Forensic Science International, 2018, 290, 207-218.	1.3	28
46	A novel route to Pt–Bi2O3 composite thin films and their application in photo-reduction of water. Inorganica Chimica Acta, 2012, 380, 328-335.	1.2	27
47	Templated growth of tungsten oxide micro/nanostructures using aerosol assisted chemical vapour deposition. Materials Letters, 2008, 62, 4582-4584.	1.3	26
48	Aerosol assisted chemical vapour deposition of gas-sensitive nanomaterials. Thin Solid Films, 2013, 548, 703-709.	0.8	26

48	548, 703-709.	0.8	26
49	Correlation of Optical Properties, Electronic Structure, and Photocatalytic Activity in Nanostructured Tungsten Oxide. Advanced Materials Interfaces, 2017, 4, 1700064.	1.9	25
50	Charge Transport Phenomena in Heterojunction Photocatalysts: The WO <sub>3</sub> /TiO <sub>2</sub> System as an Archetypical Model. ACS Applied Materials & Interfaces, 2021, 13, 9781-9793.	4.0	24
51	Single-source CVD routes to titanium phosphide. Dalton Transactions RSC, 2002, , 2702-2709.	2.3	23
52	Post-blast explosive residue – a review of formation and dispersion theories and experimental research. RSC Advances, 2014, 4, 54354-54371.	1.7	23
53	InGaN/GaN Multiple Quantum Well Photoanode Modified with Cobalt Oxide for Water Oxidation. ACS Applied Energy Materials, 2018, 1, 6417-6424.	2.5	23
54	Tungsten imido complexes as precursors to tungsten carbonitride thin films. Dalton Transactions, 2008, , 5730.	1.6	22

4

#	Article	IF	CITATIONS
55	Titanium Phosphide Coatings from the Atmospheric Pressure Chemical Vapor Deposition of TiCl4and RPH2(R =t-Bu, Ph, CyHex). Chemistry of Materials, 2002, 14, 3167-3173.	3.2	20
56	Composite thermochromic thin films: (TiO2)–(VO2) prepared from titanium isopropoxide, VOCl3 and water. Polyhedron, 2006, 25, 334-338.	1.0	20
57	p -Type PdO nanoparticles supported on n -type WO 3 nanoneedles for hydrogen sensing. Thin Solid Films, 2016, 618, 238-245.	0.8	20
58	Photocatalytic Oxygen Evolution from Cobalt-Modified Nanocrystalline BiFeO3 Films Grown via Low-Pressure Chemical Vapor Deposition from Î <sup>2</sup> -Diketonate Precursors. Crystal Growth and Design, 2016, 16, 3818-3825.	1.4	20
59	Nanoscale, conformal films of graphitic carbon nitride deposited at room temperature: a method for construction of heterojunction devices. Nanoscale, 2017, 9, 16586-16590.	2.8	20
60	Atmospheric-Pressure Chemical Vapor Deposition of Group IVb Metal Phosphide Thin Films from Tetrakisdimethylamidometal Complexes and Cyclohexylphosphine. Chemistry of Materials, 2004, 16, 1120-1125.	3.2	19
61	Heteroepitaxy of GaP on silicon for efficient and cost-effective photoelectrochemical water splitting. Journal of Materials Chemistry A, 2019, 7, 8550-8558.	5.2	19
62	Dual source atmospheric pressure chemical vapour deposition of TiP films on glass using TiCl4 and PH2But. Journal of Materials Chemistry, 2001, 11, 2408-2409.	6.7	18
63	Morphological Variations of Explosive Residue Particles and Implications for Understanding Detonation Mechanisms. Analytical Chemistry, 2016, 88, 3899-3908.	3.2	18
64	Do We Need "lonosorbed―Oxygen Species? (Or, "A Surface Conductivity Model of Gas Sensitivity in) 3509-3516.	Tj ETQq0 0 ( 4.0	) rgBT /Overlo 18
65	Gallium Phosphide photoanode coated with TiO <sub>2</sub> and CoO <sub>x</sub> for stable photoelectrochemical water oxidation. Optics Express, 2019, 27, A364.	1.7	18
66	Tungsten Oxide and Tungsten Oxide-Titania Thin Films Prepared by Aerosol-Assisted Deposition – Use of Preformed Solid Nanoparticles. European Journal of Inorganic Chemistry, 2007, 2007, 1415-1421.	1.0	17
67	Chemical vapour deposition of group Vb metal phosphide thin films. Journal of Materials Chemistry, 2003, 13, 1930.	6.7	16
68	The effect of oxygen-containing reagents on the crystal morphology and orientation in tungsten oxide thin films deposited via atmospheric pressure chemical vapour deposition (APCVD) on glass substrates. Faraday Discussions, 2007, 136, 329.	1.6	16
69	The reaction of GeCl4 with primary and secondary phosphines. Dalton Transactions, 2004, , 470.	1.6	15
70	Atmospheric Pressure Chemical Vapour Deposition of TiCl <sub>4</sub> and <i>t</i> BuAsH <sub>2</sub> to Form Titanium Arsenide Thin Films. European Journal of Inorganic Chemistry, 2010, 2010, 5629-5634.	1.0	15
71	Spectroscopic studies of sulfite-based polyoxometalates at high temperature and high pressure. Journal of Solid State Chemistry, 2012, 186, 171-176.	1.4	15
72	Chemical vapour deposition of crystalline thin films of tantalum phosphide. Materials Letters, 2003, 57, 2634-2636.	1.3	14

#	Article	IF	CITATIONS
73	Analysis of transferred fragrance and its forensic implications. Science and Justice - Journal of the Forensic Science Society, 2016, 56, 413-420.	1.3	14
74	Bis(cyclopentadienyl) zirconium(IV) amides as possible precursors for low pressure CVD and plasma-enhanced ALD. Inorganica Chimica Acta, 2010, 363, 1077-1083.	1.2	13
75	Dual-Source Atmospheric Pressure CVD of Amorphous Molybdenum Phosphide Films on Glass Using Molybdenum(V) Chloride and Cyclohexylphosphine. Chemical Vapor Deposition, 2003, 9, 10-13.	1.4	12
76	Low temperature deposition of crystalline chromium phosphide films using dual-source atmospheric pressure chemical vapour deposition. Applied Surface Science, 2004, 233, 24-28.	3.1	12
77	Single Step Solution Processed GaAs Thin Films from GaMe3andtBuAsH2under Ambient Pressure. Journal of Physical Chemistry C, 2016, 120, 7013-7019.	1.5	12
78	Robust Protection of III–V Nanowires in Water Splitting by a Thin Compact TiO <sub>2</sub> Layer. ACS Applied Materials & Interfaces, 2021, 13, 30950-30958.	4.0	12
79	A solution based route to GaAs thin films from As(NMe <sub>2</sub> ) <sub>3</sub> and GaMe <sub>3</sub> for solar cells. RSC Advances, 2015, 5, 11812-11817.	1.7	11
80	Atmospheric-Pressure CVD of Vanadium Phosphide Thin Films from Reaction of Tetrakisdimethyl-amidovanadium and Cyclohexylphosphine. Chemical Vapor Deposition, 2004, 10, 253-255.	1.4	10
81	The reaction of tin(iv) iodide with phosphines: formation of new halotin anions. Dalton Transactions, 2009, , 10486.	1.6	10
82	Titanium arsenide films from the atmospheric pressure chemical vapour deposition of tetrakisdimethylamidotitanium and tert-butylarsine. Dalton Transactions, 2011, 40, 10664.	1.6	10
83	Aerosol Assisted Chemical Vapour Deposition Synthesis of Copper(I) Oxide Thin Films for CO <sub>2</sub> Reduction Photocatalysis. Journal of Nanoscience and Nanotechnology, 2016, 16, 10112-10116.	0.9	10
84	Fragrance transfer between fabrics for forensic reconstruction applications. Science and Justice - Journal of the Forensic Science Society, 2019, 59, 256-267.	1.3	10
85	Dual-source chemical vapour deposition of titanium(III) phosphide from titanium tetrachloride and tristrimethylsilylphosphine. Applied Surface Science, 2003, 211, 2-5.	3.1	9
86	The spatial distribution patterns of condensed phase post-blast explosive residues formed during detonation. Journal of Hazardous Materials, 2016, 316, 204-213.	6.5	9
87	Persistence of transferred fragrance on fabrics for forensic reconstruction applications. Science and Justice - Journal of the Forensic Science Society, 2020, 60, 53-62.	1.3	9
88	Anisotropic Electron Transport Limits Performance of Bi <sub>2</sub> WO <sub>6</sub> Photoanodes. Journal of Physical Chemistry C, 2020, 124, 18859-18867.	1.5	9
89	Atomistic Descriptions of Gas-Surface Interactions on Tin Dioxide. Chemosensors, 2021, 9, 270.	1.8	9
90	New synthetic route to WSF4 and its solution-phase structure as determined by tungsten L(III)-edge extended X-ray absorption fine structure studies. Journal of the Chemical Society Dalton Transactions, 1996, , 2975.	1.1	8

#	Article	IF	CITATIONS
91	Micromachined Gas Sensors Based on Au-functionalized SnO 2 Nanorods Directly Integrated without Catalyst Seeds via AA-CVD. Procedia Engineering, 2016, 168, 1078-1081.	1.2	8
92	Characterization and gas sesing properties of intrinsic and Au-doped WO3 nanostuctures deposited by AACVD technique. Procedia Engineering, 2010, 5, 131-134.	1.2	7
93	CO and H2 Sensing with CVD-Grown Tungsten Oxide Nanoneedles Decorated with Au, Pt or Cu Nanoparticles. Procedia Engineering, 2012, 47, 904-907.	1.2	7
94	AACVD Grown WO <sub>3</sub> Nanoneedles Decorated With Ag/Ag <sub>2</sub> 0 Nanoparticles for Oxygen Measurement in a Humid Environment. IEEE Sensors Journal, 2019, 19, 826-832.	2.4	7
95	Direct <i>in situ</i> spectroscopic evidence of the crucial role played by surface oxygen vacancies in the O <sub>2</sub> -sensing mechanism of SnO <sub>2</sub> . Chemical Science, 2022, 13, 6089-6097.	3.7	7
96	Use of a New Non-Pyrophoric Liquid Aluminum Precursor for Atomic Layer Deposition. Materials, 2019, 12, 1429.	1.3	6
97	MOCVD of Zirconium Oxide from the Zirconium Guanidinate Complex [ZrCp′{η2-(iPrN)2CNMe2}2Cl]. ECS Transactions, 2009, 25, 561-565.	0.3	5
98	Gas-phase synthesis of hybrid nanostructured materials. Nanoscale, 2018, 10, 22981-22989.	2.8	5
99	A Multi-MOx Sensor Approach to Measure Oxidizing and Reducing Gases. Proceedings (mdpi), 2019, 14, 50.	0.2	5
100	Chemical vapour deposition (CVD) of nickel oxide using the novel nickel dialkylaminoalkoxide precursor [Ni(dmamp′) <sub>2</sub> ] (dmamp′ = 2-dimethylamino-2-methyl-1-propanolate). RSC Advances 2021, 11, 22199-22205.	s, 1 <b>.</b> 7	5
101	The Interaction between Otto Fuel II and Aqueous Hydroxylammonium Perchlorate (HAP), Part I: Initial Observations and Time-to-Event Measurements. Propellants, Explosives, Pyrotechnics, 2004, 29, 262-266.	1.0	4
102	AA-CVD growth and ethanol sensing properties of pure and metal decorated WO <sub align="right">3 nanoneedles. International Journal of Nanotechnology, 2013, 10, 455.</sub>	0.1	4
103	Single-step co-deposition of nanostructured tungsten oxide supported gold nanoparticles using a gold–phosphine cluster complex as the gold precursor. Science and Technology of Advanced Materials, 2014, 15, 065004.	2.8	4
104	Developing Nâ€Rich Carbon from C <sub>3</sub> N <sub>4</sub> â€Polydopamine Composites for Efficient Oxygen Reduction Reaction. ChemElectroChem, 2021, 8, 3954-3961.	1.7	4
105	Aerosol-assisted CVD synthesis, characterisation and gas-sensing application of gold-functionalised tungsten oxide. Journal of Sensors and Sensor Systems, 2014, 3, 325-330.	0.6	4
106	Surface Oxygen Vacancies: Dynamics of Photoâ€Induced Surface Oxygen Vacancies in Metalâ€Oxide Semiconductors Studied Under Ambient Conditions (Adv. Sci. 22/2019). Advanced Science, 2019, 6, 1970132.	5.6	3
107	Comparative study of spin-coated and vapour deposited nickel oxides for detecting VOCs. , 2020, , .		3
108	Atmospheric pressure chemical vapour deposition of vanadium arsenide thin films via the reaction of VCl4 or VOCl3 with tBuAsH2. Thin Solid Films, 2013, 537, 171-175.	0.8	2

#	Article	IF	CITATIONS
109	Sensors: Single‣tep Deposition of Au―and Ptâ€Nanoparticleâ€Functionalized Tungsten Oxide Nanoneedles Synthesized Via Aerosolâ€Assisted CVD, and Used for Fabrication of Selective Gas Microsensor Arrays (Adv. Funct. Mater. 10/2013). Advanced Functional Materials, 2013, 23, 1226-1226.	7.8	2
110	The Interaction between Otto Fuel II and Aqueous Hydroxylammonium Perchlorate (HAP), Part II: Gas Evolution and Changes in HAP Solution Acidity. Propellants, Explosives, Pyrotechnics, 2004, 29, 354-358.	1.0	1
111	Photocatalysis: Evidence and Effect of Photogenerated Charge Transfer for Enhanced Photocatalysis in WO <sub>3</sub> /TiO <sub>2</sub> Heterojunction Films: A Computational and Experimental Study (Adv. Funct. Mater. 18/2017). Advanced Functional Materials, 2017, 27, .	7.8	1
112	Deposition of tungsten oxide and silver decorated tungsten oxide for use in oxygen gas sensing. , 2017,		1
113	The Interaction between Otto Fuel II and Aqueous Hydroxylammonium Perchlorate (HAP), Part III: Depletion of Components within the Reacting Liquids. Propellants, Explosives, Pyrotechnics, 2007, 32, 222-226.	1.0	0
114	AACVD synthesis of catalytic gold nanoparticle-modified cerium(IV) oxide thin films. Physica Status Solidi C: Current Topics in Solid State Physics, 2015, 12, 996-1000.	0.8	0
115	<i>A Special Section on</i> Nanocomposites: Synthesis and Optical Related Applications.	0.9	0